Carbohydrate Polymers 84 (2011) 662–668

Carbohydrate Polymers

journal homepage: www.elsevier.com/locate/carbpol

Influence of pH on formation and properties of gellan gels

Carolina Siqueira Franco Picone, Rosiane Lopes Cunha*

Department of Food Engineering, Faculty of Food Engineering, University of Campinas (UNICAMP), Rua Monteiro Lobato, 80, 13083-862 Campinas, SP, Brazil

ARTICLE INFO

Article history:
Received 23 July 2010
Received in revised form 7 December 2010
Accepted 16 December 2010
Available online 22 December 2010

Keywords:
Gellan gum
Acidification
Rheology
Coil–helix transition

ABSTRACT

The effect of pH (3.5, 5.3 and 7.0) on the formation of deacylated gellan gels was studied using oscillatory shear measurements and microcalorimetric trials in heating–cooling cycles at 1 °C min^{-1}. In addition, the mechanical properties and structure of the gels formed at the different pH values were evaluated by uniaxial compression and scanning electron microscopy, respectively. An increase in pH led to an increase in temperature and decrease in enthalpy of the coil–helix transition. These results were attributed to a decreased formation of junction zones at higher pH values due to greater electrostatic repulsion between the gellan molecules. As a consequence, gels formed at neutral pH were more fragile and deformable than acid gels. All the samples showed thermo-reversible rheological behavior, presenting the same rheological properties at 20 °C, before and after heating to 90 °C.

1. Introduction

Gellan gum is a linear anionic heteropolysaccharide produced by *Sphingomonas elodea* (Nishinari, 1999), which has been a subject of interest since its discovery in 1980 due to its ability to form transparent gels even at low concentrations (Rodríguez-Hernández, Durand, Garnier, Tecante, & Doublier, 2003). In addition, traditional gelling agents such as agarose and carrageenan show reduced gelling capacity at low pH, whereas gellan gum can form strengthened gels (Moritaka, Nishinari, Taki, & Fukuba, 1995; Yamamoto & Cunha, 2007).

As with other polysaccharides, gellan molecules undergo a coil to double-helix transition with decreasing temperature, which may lead to gel formation depending on the ionic strength and pH of the solution. The gelation process is known to consist of two steps (Milas & Rinaudo, 1996). Firstly the gellan coil molecules form double helices with the reduction in temperature, and secondly, these helices aggregate forming junction zones, resulting in system gelation (Yuguchi, Urakawa, & Kajiwara, 1997). In water, at low ionic strength and neutral pH, aggregation of the helices is impeded by the electrostatic repulsion between negatively charged carboxylic groups on the gellan. The addition of salt or reduction in pH decreases intermolecular repulsion between the helices enhancing junction zone formation and consequently, the gel strength (Funami et al., 2008; Yamamoto & Cunha, 2007). The role of salt ions in gel formation has been widely studied (Fukada et al., 2002; Funami et al., 2008; Milas & Rinaudo, 1996; Miyoshi, Takaya, & Nishinari, 1996; Moritaka, Nishinari, Nakahama, & Fukuba, 1992; Moritaka et al., 1995). In the presence of salt ions, the gelling and melting temperatures of gellan gels shift to higher temperatures and the number of junction zones is enhanced. This makes the gel more heat resistant and leads to an increase in the gel elastic modulus and rigidity. However, only a small number of studies (Horinaka, Kania, Horib, & Maeda, 2004; Mao, Tang, & Swanson, 1999; Moritaka et al., 1995; Yamamoto & Cunha, 2007) were concerned about the effect of pH on the gel properties. The aim of the present work was to study the effect of pH on the gellan coil–helix transition using rheological and calorimetric techniques, so as to evaluate any influence on the mechanical and structural properties of the gels.

2. Material and methods

2.1. Material

Deacylated gellan gum powder (Kelcogel® F) (3.42% w/w moisture content) was kindly donated by Kelco Biopolymers (San Diego, CA). The ions content of the gellan, as determined by Inductively Coupled Plasma (ICP) Emission Spectroscopy (Perkin Elmer – Optima 3000 DV, Waltham, MA, USA) was (%, w/w): K^+ = 4.13, Na^+ = 0.43 and Ca^{2+} = 0.18. The stoichiometric equivalence to the carboxyl groups for 1.5% (w/w) gellan solution was (%): K^+ = 38.36, Na^+ = 6.52 and Ca^{2+} = 3.74. Lactic acid was purchased from Merck (Germany).

2.2. Preparation of the gellan solutions

The solution of 1.5% (w/w) gellan gum was prepared by stirring the gellan powder in deionized water at 80 °C for 30 min in a jacketed vessel. The pH was adjusted to 7.0 ± 0.2 and 3.5 ± 0.2 by the

* Corresponding author. Tel.: +55 19 3521 4047; fax: +55 19 3521 4027.
E-mail address: rosiane@fea.unicamp.br (R.L. Cunha).

0144-8617 © 2010 Elsevier Ltd. Open access under the Elsevier OA license.
doi:10.1016/j.carbpol.2010.12.045

addition of 0.02 M NaOH or 0.2 M lactic acid, respectively. Solutions at the natural pH (5.3 ± 0.2) were also evaluated. The content of Na^+ ions added was much lower than the ion content of the raw material. The content of K^+ was kept constant since gellan concentration was the same for all the samples. The potassium concentration in the raw material probably contributed to a partial network formation, but not for the further differences observed in rheological and DSC thermal behavior between the samples.

For the thermal and rheological measurements, the solutions were analyzed just after preparation at 80 °C. For the analyses of the mechanical properties and microstructure, the gellan solutions were poured into cylindrical plastic tubes previously lubricated with silicon oil (21 mm inner diameter × 21 mm height) and Petri dishes, which were cooled to 10 °C in an ice bath. The gels were then maintained at the same temperature (10 °C) for 24 h in order to assure complete gel formation.

2.3. Oscillatory rheology

The rheological behavior of the samples was evaluated by oscillatory shear measurements in a stress-controlled rheometer (Carri–Med CSL^2 500, TA Instruments, UK) equipped with a stainless steel cone and plate geometry (cone angle = 1.59°; cone diameter = 60 mm). The samples were transferred onto the rheometer plate (which was preheated at 60 °C) immediately after the heat treatment, and were then quickly heated to 90 °C using a Peltier unit. To avoid sample evaporation, the cone and plate was surrounded by a fine layer of silicon oil. The samples were then homogenized by pre-shearing at 100 s^{-1} for 2 min and allowed to rest for 5 min prior to the measurements. As the samples were totally liquid at such temperature, no rim instability or structure damage was observed in the samples. Three sweeps (cooling–heating–cooling) were carried out between 20 and 90 °C at 1 °C min^{-1}, 0.1 Hz and 0.5 Pa. Changes in the slope of complex viscosity vs. temperature curves were maximized from the derivation of the data using the Savitzky & Golay filter (Savitzky & Golay, 1964). The temperatures of rheological transitions were determined by the maxima in the (absolute) slope of $\log(\eta^*)$. The contribution of the elastic (G') and loss (G'') moduli on these rheological changes were evaluated by $\tan\delta$ (G''/G'). The gel point was determined using the criterion of crossover between the G' and G'' (Yamamoto & Cunha, 2007).

2.4. Thermal behavior

The thermal behavior of samples was measured using a VP-DSC (MicroCal, Northampton, MA) calorimeter equipped with twin 0.542 ml cells for the reference and sample solutions. The samples were loaded at 60 °C and heated to 90 °C before the test. Four repeated cooling–heating cycles between 90 and 5 °C were carried out at 1 °C min^{-1}. The reference thermogram was recorded under the same conditions by filling both cells with water. The transition temperature (T_{peak}) was determined as the temperature of the maximum peak, whereas the enthalpy was calculated from the area enclosed by the peak and the baseline.

2.5. Compression testing

The mechanical properties of the gels at the different pH values were determined by uniaxial compression measurements in a TA-XT Plus Texture Analyser (Stable Microsystems Ltd., Surrey, England), equipped with a 40 mm diameter cylindrical acrylic plate lubricated with silicon oil to minimize friction between the sample and the probe. The gels were compressed to 80% of their original height at 10 °C, using a crosshead speed of 1 mm/s.

Hencky stress (σ_H) and strain (ε_H) were calculated from the force-deformation data according to Eqs. (1) and (2), respectively (Steffe, 1996):

$$\sigma_H = F(t)\left[\frac{H(t)}{H_0 A_0}\right] \quad (1)$$

$$\varepsilon_H = -\ln\left[\frac{H(t)}{H_0}\right] \quad (2)$$

where $F(t)$ is the force at time t, A_0 and H_0 are the initial sample area and height, respectively, and $H(t)$ is the height at time t.

The stress (σ_r) and strain (ε_r) at fracture were obtained from the maximum point of the stress–strain curve, whilst the Young's modulus (E) was the slope of the initial linear region of this curve (up to 1% of deformation).

2.6. Scanning electron microscopy

Pieces of gel (approximately 10 mm × 2 mm × 2 mm) were fixed overnight in 2.5% glutaraldehyde in cacodylate buffer (0.1 M) at pH 7.2. After rinsing in cacodylate buffer (0.1 M), the samples were fractured in liquid nitrogen, followed by another rinse with cacodylate buffer. The fractured samples were post fixed overnight in 1% buffered osmium tetroxide and then dehydrated in a graded ethanolic series (30, 50, 70, 90 and 100%, v/v). In order to avoid structural damage, the samples were dried at the CO_2 critical point (Balzers Critical Point Dryer CPD03) and then mounted on aluminum stubs and coated with gold in a SCD 050-Balzer Sputter Coater. At least three images of typical structures were recorded at a magnification of ×1.000 using a JEOL JSM 5800 LV (Tokyo, Japan) microscope operating at 10 kV.

2.7. Statistical analyses

The results were evaluated from triplicates of each sample, using the analysis of variance (ANOVA). The significant differences ($p < 0.05$) between different samples were determined by the Tukey procedure, using the software STATISTICA 5.5 (Statsoft Inc., Tulsa, USA).

3. Results

3.1. Thermal scanning rheology

Fig. 1 shows the rheological behavior of sample during heating–cooling cycles. The mainly points were obtained within the linear viscoelastic region of samples (with no structural damage), except by the points at high temperatures (low viscosity and non-gel formation). As the measurements were carried out using stress controlled operation mode and the sample showed great changes in viscosity and elasticity values, part of the test would certainly be out of linear viscoelastic range. However, it did not damaged the sample structure, since in such case the transition temperatures during cooling and G' G'' crossover should be lower than the determined by DSC, which did not occur.

A single increase in complex viscosity was observed during cooling (Fig. 1), which reflected in a decrease in $\tan(\delta)$ values. Such phenomenon occurred at slightly higher temperatures as the pH increased (Table 1), but the gel point temperature (Table 2) did not vary with the pH in both two cooling cycles. Such temperatures are in agreement with the results obtained by Miyoshi et al. (1996).

However, different complex viscosity profiles were observed on heating, depending on the pH (Fig. 1) and relevant hysteresis. Hysteresis is identified as the difference between the ascending (sol to gel transition) and descending (gel to sol transition) curves (Funami et al., 2008). All the curves for η^* presented four slope changes,

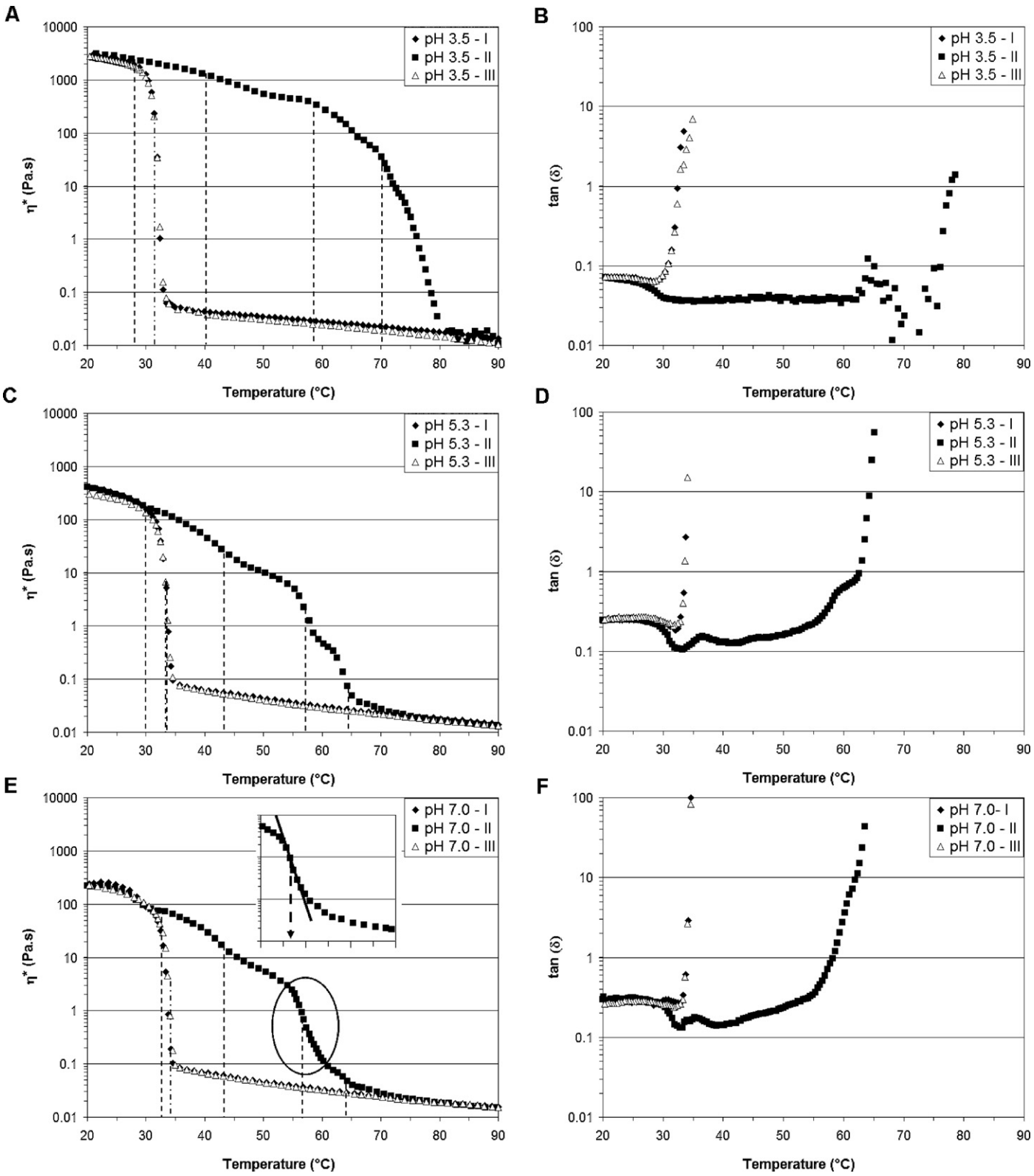

Fig. 1. Complex viscosity (η^*) in cooling–heating cycles (20–90 °C) of gellan gum 1.5% (w/w) (A) pH 3.5, (B) pH 5.3 and (C) pH 7.0. (···) Transition temperatures on cooling; (- - -) transition temperatures on heating. I. First cooling, II. Heating, III. Second cooling. The inset shows the method used to determine the transitions.

some of which were very pronounced and others not so easy to identify (Table 1 and Fig. 1). At pH 3.5, the increase in temperature led to a decrease in complex viscosity from 3000 Pa s (at 20 °C) to 0.01 Pa s near 80 °C. At such a pH value, the first transition occurred at a temperature below 30 °C and the last one at 70 °C (temperature variation of about 40 °C) (Table 1 and Fig. 1). Increasing the solution pH to 5.3, the first two transitions occurred at higher temperatures than at pH 3.5 whilst the others were observed at lower temperatures. The same tendencies were observed at pH 7.0 (Table 1 and Fig. 1). Slope changes in the determination of the rheological

Table 1
Transition temperatures of the complex viscosity changes for 1.5% (w/w) gellan solutions at pH 3.5, 5.3 and 7.0 during consecutive cooling–heating cycles.

	Transition	Transition temperature (°C)		
		pH 3.5	pH 5.3	pH 7.0
Cooling I	1st	31.4 ± 0.5^{Aa}	33.6 ± 0.9^{Ba}	34.2 ± 0.6^{Ca}
Heating	1st	28.1 ± 0.3^{Ab}	29.9 ± 0.6^{Bb}	32.8 ± 0.6^{Ca}
Heating	2nd	40.1 ± 0.8^{Ac}	43.3 ± 0.5^{Bc}	43.3 ± 0.6^{Bb}
Heating	3rd	58.6 ± 0.3^{Ad}	57.2 ± 0.2^{Bd}	56.7 ± 0.3^{Cc}
Heating	4th	70.1 ± 0.5^{Ae}	64.7 ± 0.8^{Be}	64.1 ± 0.3^{Bd}
Cooling II	1st	31.4 ± 0.5^{Aa}	33.4 ± 0.8^{Ba}	34.1 ± 0.5^{Ba}

$F(17,36) = 1915.3$, $p = 0.00$. Different capital letters in the same row and small letters in the same column mean statistically significant differences ($p < 0.05$).

properties during the thermal scanning analysis were previously reported by Miyoshi et al. (1996), who studied the effect of gellan concentration on the rheological properties of gellan gum solutions prepared without variation in pH. They only observed two different slope changes, which were attributed to the helix–coil transition followed by the sol–gel transition.

Overall the tan δ showed a decrease around 33 °C on heating which was more pronounced at higher pH values. Such a decrease was associated to the higher G'' depression as compared to G'. Above 60 °C tan δ increased abruptly, due to the sharp decrease of G' (Fig. 1B, D and F). The hysteresis between the cooling and heating scans (Fig. 1) decreased as the pH increase, suggesting that a more lightly cross-linked network was formed with a smaller number of aggregated helices. Previous findings related the increase in hysteresis to the decrease in acyl content of the gellan gum molecules and the presence of gel-promoting cations, which enhance molecular associations (Funami et al., 2008; Gunning, Kirby, Ridout, Brownsey, & Morris, 1996; Morris, Kirby, & Gunning, 1999). In the present case, the gellan gum used was totally deacylated (NutraSweet Kelco Company, 1996), and thus the changes in hysteresis were associated with interactions promoted by lower pH values and the cations presence. As well as the effect of cation addition, the reduction in pH increased the concentration of positive ions in solution, screening electrostatic repulsion between helices and favoring helix–helix association by way of hydrogen bonds, resulting in an increase in thermal stability or hysteresis of the samples.

3.2. DSC

Fig. 2 shows the DSC thermograms of the samples at different pH values. The number of peaks remained the same after consecutive cooling–heating cycles. The cooling curves showed a single exothermic peak for all pH values, whilst up to four endothermic peaks were observed on the heating curves. These results were in good agreement with those obtained by Moritaka et al. (1995) and Tanaka and Nishinari (2007). The first endothermic peak appeared in the same temperature range as the exothermic peak observed on cooling, but was significantly smaller and became larger with increases in the pH value (Fig. 2). An overlap of endothermic peaks was detected around 33–50 °C, which became broader as the pH

Table 2
Temperatures of G' and G'' crossover for 1.5% (w/w) gellan solutions at pH 3.5, 5.3 and 7.0 during consecutive cooling–heating cycles.

	Onset temperature (°C)		
	pH 3.5	pH 5.3	pH 7.0
Cooling I	32.4 ± 0.7	33.3 ± 0.5	33.5 ± 0.3
Cooling II	32.9 ± 0.6	33.4 ± 0.7	34.0 ± 0.5

There is no statistically significant differences between the means ($F(5,12) = 1.76$, $p = 0.20$).

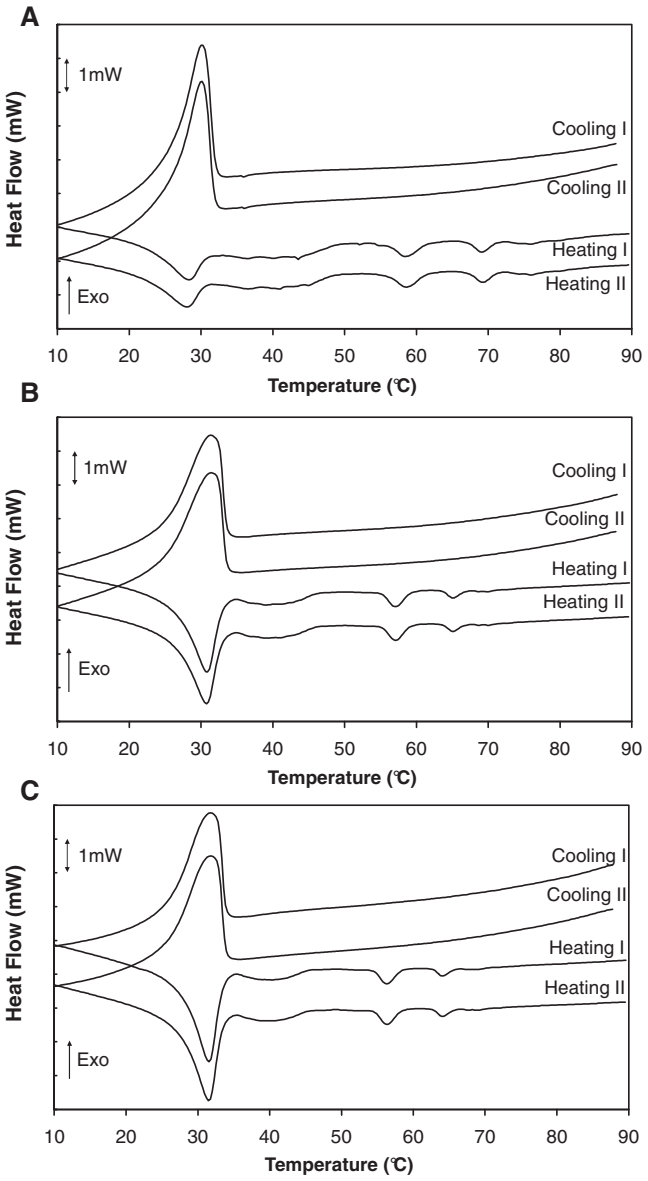

Fig. 2. DSC-thermograms of 1.5% (w/w) gellan solutions at (A) pH 3.5, (B) pH 5.3 and (C) pH 7.0, with a heating rate of 1 °C/min.

decreased, making it impossible to determine all the peak temperatures and enthalpies at pH 3.5. Two more peaks were detected on heating at higher temperatures, which shifted to lower temperatures as the pH increased. The second endothermic peak also shifted to lower temperatures as the pH increased from 5.3 to 7.0, but the opposite tendency was observed with the first peak. Table 3 shows an increase in the first peak temperature of about 3 °C and Table 4 a strong increase in enthalpy when the pH changed from 3.5 to 7.0. In the same way, the temperature of the exothermic cooling peaks also increased as the pH rose, but no significant changes in enthalpy were observed (Table 4). For all the samples, the sum of the endothermic enthalpy values was slightly lower than the enthalpy of the single exothermic peak observed on cooling (Table 4), especially at the lowest pH. It suggests that the second peak may be partially overlapping the first peak making difficult to establish the baseline for integration of each peak. Indeed the first peak became broader and presented a reduced enthalpy at lower pH values. Moreover, the small peaks observed at pH 3.5 hinder the establishment of the baseline, which probably masked some part of total enthalpy associated to the thermal transitions.

Table 3
Peak temperatures of thermograms for 1.5% (w/w) gellan solutions at pH 3.5, 5.3 and 7.0 during consecutive cooling–heating cycles.

	Peak temperature (°C)		
	pH 3.5	pH 5.3	pH 7.0
Cooling I	30.29 ± 0.25^{Aa}	31.26 ± 0.28^{Ba}	31.70 ± 0.04^{Bae}
Heating I Peak1	28.45 ± 0.09^{Ab}	30.78 ± 0.15^{Bab}	31.57 ± 0.01^{Cae}
Heating I Peak2	–	40.72 ± 0.05^{Ac}	39.83 ± 0.28^{Bb}
Heating I Peak3	58.80 ± 0.17^{Ac}	57.13 ± 0.19^{Bd}	56.33 ± 0.00^{Cc}
Heating I Peak4	68.79 ± 0.30^{Ad}	64.85 ± 0.19^{Be}	64.05 ± 0.00^{Cd}
Cooling II	30.35 ± 0.18^{Aa}	$31.41 \pm 0.27\ A^{Baf}$	31.77 ± 0.07^{Bae}
Heating II Peak 1	28.14 ± 0.10^{Ab}	30.63 ± 0.12^{Bbf}	31.39 ± 0.07^{Ca}
Heating II Peak 2	–	40.81 ± 0.06^{Ac}	40.17 ± 0.46^{Ab}
Heating II Peak 3	58.75 ± 0.17^{Ac}	56.98 ± 0.17^{Bd}	56.41 ± 0.08^{Bc}
Heating II Peak 4	69.00 ± 0.30^{Ad}	64.88 ± 0.26^{Be}	64.27 ± 0.05^{Bd}

Different capital letters in the same row and small letters in the same column mean statistically significant differences ($p < 0.05$). $F(27,56) = 19{,}000$; $p = 0.00$.

Table 4
Enthalpy values for 1.5% (w/w) gellan solutions at pH 3.5, 5.3 and 7.0 during consecutive cooling–heating cycles. Negative sign means exothermic transition.

	Peak enthalpy (kJ/g)		
	pH 3.5	pH 5.3	pH 7.0
Cooling I	-13.52 ± 0.83^{Aa}	-12.03 ± 1.10^{Aa}	-12.44 ± 0.36^{Aa}
Heating I Peak1	3.07 ± 0.25^{Ab}	6.60 ± 0.46^{Bb}	6.86 ± 0.14^{Bb}
Heating I Peak2	–	2.63 ± 0.26^{Ac}	3.38 ± 0.65^{Ac}
Heating I Peak3	2.24 ± 0.10^{Ac}	0.96 ± 0.52^{Bd}	0.67 ± 0.03^{Bd}
Heating I Peak4	0.73 ± 0.13^{Ad}	0.26 ± 0.03^{Bd}	0.32 ± 0.01^{Bd}
Cooling II	-12.83 ± 0.47^{Aa}	-11.64 ± 0.06^{Aa}	-12.94 ± 0.22^{Aa}
Heating II Peak 1	2.75 ± 0.13^{Abe}	6.59 ± 0.65^{Bb}	6.72 ± 0.14^{Bb}
Heating II Peak 2	–	2.79 ± 0.34^{Ac}	3.41 ± 1.31^{Ac}
Heating II Peak 3	2.04 ± 1.24^{Ace}	0.68 ± 0.03^{Bd}	0.73 ± 0.02^{Bd}
Heating II Peak 4	0.57 ± 0.01^{Ad}	0.26 ± 0.03^{Bd}	0.33 ± 0.00^{Bd}

Different capital letters in the same row and small letters in the same column mean statistically significant differences ($p < 0.05$). $F(27,56) = 505{,}7$; $p = 0.00$.

The re-cooling and re-heating did not affect the temperature and enthalpy of the peaks (Tables 3 and 4) showing the thermal reversibility of the gellan gels.

Overall, peak temperatures showed good agreement with the temperature transitions observed on rheological tests (Tables 1 and 3), despite of the different thermal history of both measurements.

3.3. Compression testing

The uniaxial compression results showed an increase in gel hardness and elasticity as the pH decreased (Figs. 3 and 4A and C), in agreement with the results obtained by Yamamoto and Cunha (2007). As the pH increased, so the curves became broader

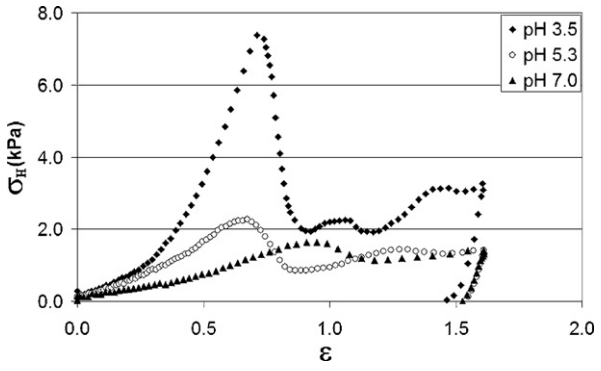

Fig. 3. Typical strain–stress curves for 1.5% (w/w) gellan gels at pH 3.5, 5.3 and 7.0.

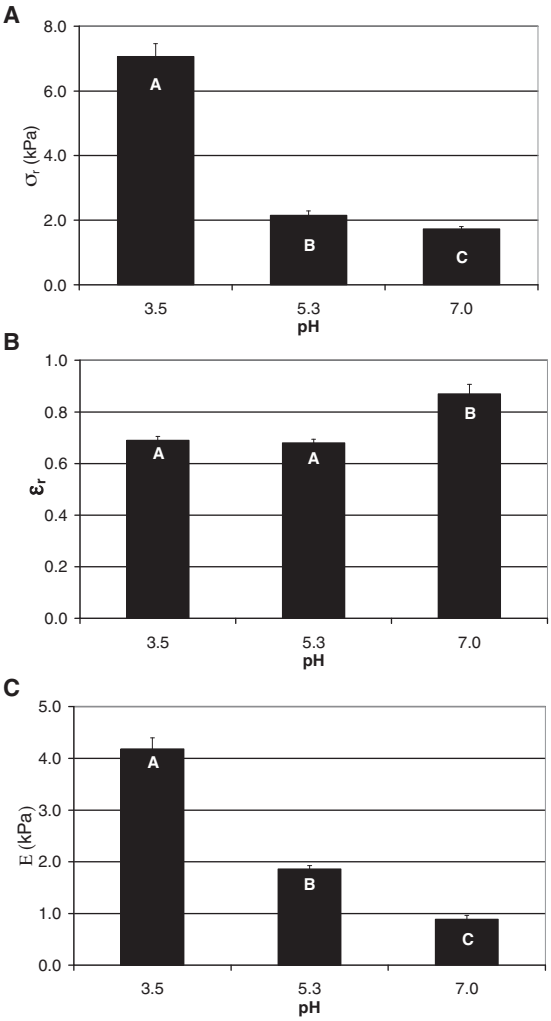

Fig. 4. Mechanical properties of gels of 1.5% (w/w) gellan gum at pH 3.5, 5.3 and 7.0. (A) Stress at fracture (σ_r), (B) strain at fracture (ε_r) and (C) Young's modulus (E). Means and error bars were calculated from triplicates of each sample. Means with different letters show statistically significant differences at $p < 0.05$.

(Fig. 3) and the rupture stress of the gels at pH 3.5 was more than twice that obtained at the other pH values (Figs. 3 and 4). However, the deformation at fracture or deformability showed the opposite tendency (Figs. 3 and 4B). The strain at fracture of the gels at pH 3.5 and 5.3 were statistically the same, and both were lower than that at pH 7.0. After the rupture point, the curves presented squelching of the samples. In this region, the gels at pH 3.5 showed a number of small fractures, which decreased as the pH increased.

3.4. Microscopy

Fig. 5 shows the microstructures of the gels at the different pH values. Overall the micrographs showed very compact structures with a great number of pores, typical of gellan gum networks (de Jong & Van de Velde, 2007; Picone & Cunha, 2010; Yamamoto & Cunha, 2007). Acidification seemed to close the pore network. The gels at pH 7.0 presented a flat and closed network, whilst those at pH 5.3 were more continuous and with less pores (Fig. 5B and C). At pH 3.5 the network was even more continuous and with smaller pores, which were homogeneously distributed throughout the structure (Fig. 5A).

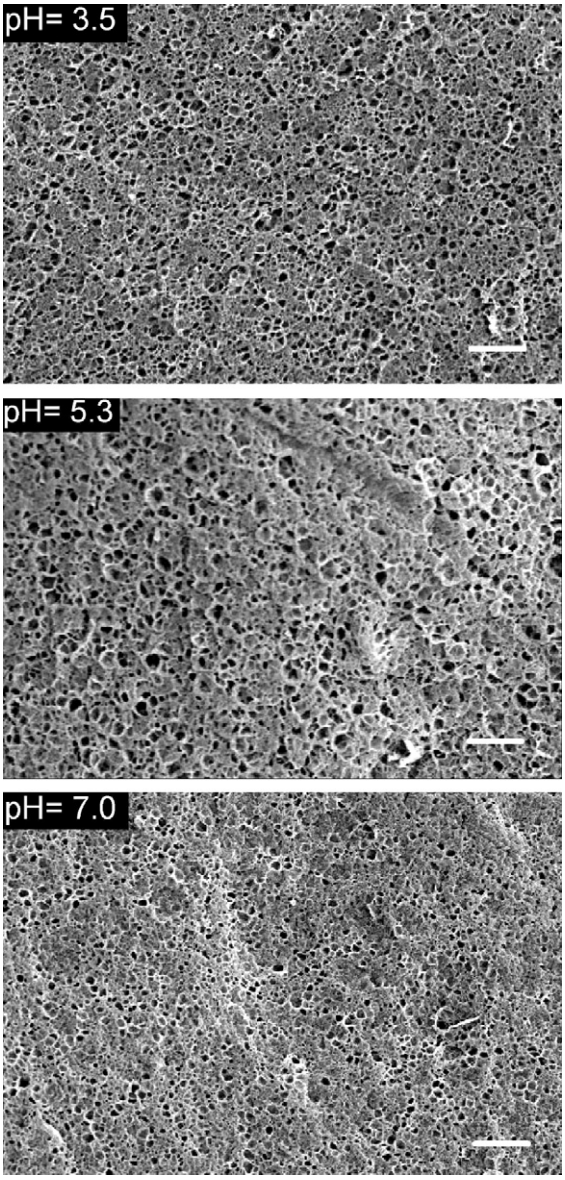

Fig. 5. SEM micrographs of 1.5% (w/w) gellan gum gels at pH 3.5, 5.3 and 7.0. Scale bar = 10 μm.

4. Discussion

The gelation of gellan is known to occur during cooling by way of the coil–helix conformational transition followed by an association between the helices, resulting in network formation. Independent of pH, the complex viscosity of the gellan solutions increased in a single step during the cooling ramp (Fig. 1), and their transition temperatures were similar than the gel point. This suggests that as soon as the helices were formed, the sol–gel transition took place due to molecular association. The gelation process occurred in a single step, as confirmed by the DSC results in which a single exothermic peak was observed (Fig. 2). The rheological and DSC results suggested that such phenomena occurred at slightly lower temperatures at acid pH values (Tables 1 and 3), which was attributed to the more compact and denser gel structure formed at pH 3.5 (Fig. 5), requiring more time and energy to complete the network formation. Hysteresis between the cooling–heating rheological scans was also more pronounced at lower pH, which could be associated with the greater stability of the aggregated helices formed under acid conditions, as compared with the isolated double helices. Moreover, hysteresis was previously reported to be related to the continuousness and homogeneity of the gel network structure (Funami et al., 2008), which was confirmed by the more continuous and less porous structure observed at pH 3.5 (Fig. 5).

All the samples showed thermo-reversible behavior, since the gel point values were statistically the same after heating and re-cooling, independent of the sample pH value (Table 2). However the calorimetric measurements showed differences in peak shape, temperature and enthalpy (Fig. 2), whilst different hysteresis and slopes were observed at similar temperatures in the thermal rheological scans (Fig. 1) according to the pH values of the samples. Besides of the different thermal history between the rheological and DSC measurements, the transition temperatures obtained from both techniques showed a good agreement on cooling and heating, especially at high temperatures. If the thermal history had affected the structure formation, it would be expected an increase in transition temperatures of DSC measurements as compared to rheological tests. As it did not happened, we considered that the difference in thermal history caused by the decrease up to 5 or 20 °C (with no holding time) did not affect significantly the observed transitions and that the applied shear fields of rheological tests were not strong enough to affect the thermally induced structural changes.

Overall, all the samples showed four peaks in the rheological and DSC scans (Figs. 1 and 2), and some authors have suggested that these peaks can be related to the presence of junction zones of different thermo stability (Moritaka et al., 1995; Nishinari, 1997). We believe that the first transition on heating (larger peak) corresponded to the melting of non-aggregated helices. The enthalpy values increased with increasing pH, indicating that more helices remained non-aggregated and less junction zones had been formed, considering that the electrostatic repulsion between gellan carboxyl groups tended to increase. Such a phenomenon was observed in both techniques at similar temperatures (Figs. 1 and 2 and Tables 1 and 3). This assumption was confirmed by $\tan\delta$ results that showed a decrease near 30 °C, because of the decrease in G'' (decrease of non-aggregated helices density).

The second transition was, in fact an overlapping of peaks resulting from the break of double helix structures. The other peaks observed were related to the melting of these aggregated helices and disruption of junction zones with different thermo stabilities (Figs. 1 and 2) formed by presence of different ions and varied H^+ ions content. The enthalpy and temperature of such peaks decreased with increasing pH (Tables 3 and 4), since less intermolecular interactions were established at higher pH values. As a consequence, slope changes of the complex viscosity as a function of temperature were also observed at similar temperatures (Table 1). This occurred because the double helical gellan molecules have a higher relative viscosity than the more flexible disordered form, as previously reported by Lee and Brant (2002) for xanthan, a polysaccharide presenting a similar conformational transition (helix–coil).

The higher values for complex viscosity observed at lower pH values and 20 °C, resulting from greater molecular association, reflected directly on the gel mechanical properties and microstructure (Figs. 3 and 4). During the uniaxial compression measurements the force applied was better distributed along the network structure of the acid gels, showing higher stress at fracture and elasticity modulus values (Fig. 4A and C). However, since the network was more compact, the mobility of the gel strands under the application of force was reduced, resulting in less deformable gels (Fig. 4B).

5. Conclusion

Although the gellan gels were thermo reversible, independent of pH, their formation and mechanical properties were shown to be

directly dependent on the solution pH. An increase in pH led to the formation of a reduced number of junction zones and a decrease in molecular aggregation, reducing gel rigidity. On the other hand, this structure increased gel deformability, since the mobility of the strands increased. Thermal scanning showed that the gels were formed by junction zones with different thermal stabilities due to the presence of different H^+ concentration and the other ions present in the raw material. The disruption of such interactions on heating occurred in four steps, leading to different slopes for the complex viscosity as a function of temperature. The DSC analyses together with the thermal rheological scans were shown to be a powerful tool in understanding the type of gellan network structure, as previously reported for other polysaccharide gels.

Acknowledgements

The authors are grateful to Dr. Watson Loh and Dr. Fernanda Rosa Alves for their cooperation in the DSC experiments. This work was supported by The Fundação de Amparo à Pesquisa e Desenvolvimento de São Paulo–Brazil (FAPESP, Grant Nos. 2004/08517-3 and 2006/02390-7) and by The Conselho Nacional de Desenvolvimento Científico e Tecnológico – Brazil (CNPq, Grant No. 301869/2006-5).

References

de Jong, S., & Van de Velde, F. (2007). Charge density of polysaccharide controls microstructure and large deformation properties of mixed gels. *Food Hydrocolloids*, *21*, 1172–1187.

Fukada, H., Takahashi, K., Kitamura, S., Yuguchi, Y., Urakawa, H., & Kajiwara, K. (2002). Thermodynamics and structural aspect of the gelling process in the gellan gum/metal salt aqueous solutions. *Journal of Thermal Analysis and Calorimetry*, *70*, 797–806.

Funami, T., Noda, S., Nakauma, M., Ishihara, S., Takahashi, R., Al-Assaf, S., et al. (2008). Molecular structures of gellan gum imaged with atomic force microscopy in relation to the rheological behavior in aqueous systems in the presence or absence of various cations. *Journal of Agricultural and Food Chemistry*, *56*, 8609–8618.

Gunning, A. P., Kirby, A. R., Ridout, M. J., Brownsey, G. J., & Morris, V. J. (1996). Investigation of gellan networks and gels by atomic force microscopy. *Macromolecules*, *29*, 6791–6796.

Horinaka, J., Kania, K., Horib, Y., & Maeda, S. (2004). Effect of pH on the conformation of gellan chains in aqueous systems. *Biophysical Chemistry*, *111*, 223–227.

Lee, H., & Brant, D. A. (2002). Rheology of concentrated isotropic and anisotropic xanthan solutions: 3. Temperature dependence. *Biomacromolecules*, *3*, 742–753.

Mao, R., Tang, J., & Swanson, B. G. (1999). Effect of pH buffers on mechanical properties of gellan gels. *Journal of Texture Studies*, *30*, 151–166.

Milas, M., & Rinaudo, M. (1996). The gellan sol–gel transition. *Carbohydrate Polymers*, *30*, 177–184.

Miyoshi, E., Takaya, T., & Nishinari, K. (1996). Rheological and thermal studies of gel–sol transition in gellan gum aqueous solutions. *Carbohydrate Polymers*, *30*, 109–119.

Moritaka, H., Nishinari, K., Nakahama, N., & Fukuba, H. (1992). Effects of potassium chloride and sodium chloride on the thermal properties of gellan gum gels. *Bioscience, Biotechnology, and Biochemistry*, *56*, 595–599.

Moritaka, H., Nishinari, K., Taki, M., & Fukuba, H. (1995). Effects of pH, potassium chloride, and sodium chloride on the thermal and rheological properties of gellan gum gels. *Journal of Agricultural and Food Chemistry*, *43*, 1685–1689.

Morris, V. J., Kirby, A. R., & Gunning, A. P. (1999). A fibrous model for gellan gels from atomic force microscopy studies. *Progress in Colloid and Polymer Science*, *114*, 102–108.

Nishinari, K. (1997). Rheological and DSC study of sol–gel transition in aqueous dispersions of industrially important polymers and colloids. *Colloid and Polymer Science*, *275*, 1093–1107.

Nishinari, K. (1999). *Physical chemistry and industrial application of gellan gum*. Berlin: Springer.

NutraSweet Kelco Company. (1996). *Gellan gum* (3rd ed.). San Diego, CA: NutraSweet Kelco Co.

Picone, C. S. F., & Cunha, R. L. (2010). Interactions between milk proteins and gellan gum in acidified gels. *Food Hydrocolloids*, *24*, 502–511.

Rodríguez-Hernández, A. I., Durand, S., Garnier, C., Tecante, A., & Doublier, J. L. (2003). Rheology-structure properties of gellan systems: Evidence of network formation at low gellan concentrations. *Food Hydrocolloids*, *17*, 621–628.

Savitzky, A., & Golay, M. J. E. (1964). Smoothing and differentiation of data by simplified least squares procedures. *Analytical Chemistry*, *36*, 1627–1639.

Steffe, J. F. (1996). *Rheological methods in food process engineering*. East Lansing: Freeman Press.

Tanaka, S., & Nishinari, K. (2007). Unassociated molecular chains in physically crosslinked gellan gels. *Polymer Journal*, *39*, 397–403.

Yamamoto, F., & Cunha, R. L. (2007). Acid gelation of gellan: Effect of final pH and heat treatment conditions. *Carbohydrate Polymers*, *68*, 517–527.

Yuguchi, Y., Urakawa, H., & Kajiwara, K. (1997). Structural characteristics of crosslinking domain in gellan gum gel. *Macromolecular Symposia*, *120*, 77–89.